BLE-based Power Efficient WSN for Industrial IoT Train Integrity Monitoring

1st Nick De Raeve
Dept. of Information Technology
Ghent University - imec, IDLab
Ghent, Belgium
nick.deraeve@ugent.be

2nd Jo Verhaevert
Dept. of Information Technology
Ghent University - imec, IDLab
Ghent, Belgium
jo.verhaevert@ugent.be

3th Patrick Van Torre
Dept. of Information Technology
Ghent University - imec, IDLab
Ghent, Belgium
patrick.vantorre@ugent.be

4th Frederick Ronse
Ovinto
Aalter, Belgium
frederick.ronse@ovinto.com

5th Hendrik Rogier
Dept of Information Technology
Ghent University - imec, IDLab
Ghent, Belgium
hendrik.rogier@ugent.be

***Abstract*—Monitoring train integrity is a very important topic for economical, management and safety reasons. Knowing the localization, volume and other parameters is very valuable for most train and large industry companies. Current literature focuses on placing many sensors in a Wireless Sensor Network (WSN) around the train wagons, but do not take battery lifetime into perspective. With the increasing interest in industrial Internet of Things (IoT) applications, the connectivity and battery lifetime are very important parameters. In this paper, the vibrations measured on train wagons are analyzed in order to find the most optimal trigger point to wake up or to put the WSN in a deep sleep mode. This way, a large amount of power can be saved and extend the battery lifetime significantly. Furthermore, several Received Signal Strength Indicator (RSSI) measurements were performed to find the optimal Tx level and antenna topology for communication between different wireless sensor nodes on the train wagon. The proposed measurements show that an inexpensive accelerometer and a prefabricated antenna are perfectly usable in the WSN. RF measurements on the brakes results in an average Package Receive Rate (PRR) of approximately $92\,\%$ and an Average Received Power (ARP) of around $-83\,\mathrm{dBm}$ starting from a Tx level of $4\,\mathrm{dBm}$.**

***Index Terms*—BLE, RSSI, Package Receive Rate, Average Received Power, PIFA, accelerometer, train wagon, train integrity, Radio-frequency identification.**

I. Introduction

MONITORING train integrity is a very important topic for economical, management and safety reasons. Knowing where a train and/or train wagons are located, how much freight they are carrying, the condition of the brakes, etc. can save the company a lot of money. Furthermore, having a real-time track and trace of these trains and train wagon parameters will increase the ease of use and maintenance significantly.

In literature, extensive research is performed in developing Wireless Sensor Network (WSN) inside [1] and outside [2], [3] train wagons [4], based on different communication protocols [5]. A typical WSN consists of several Sensor Nodes (SNs) spread across a train wagon and transfer their data to the Central Node (CN), some of these sensors have an integrated energy harvester [6], [7]. In a later step, these WSN can be connected in an industrial Internet of Things (IoT) network. This paper describes acceleration and RF measurements performed on train wagons in an industrial environment based on Bluetooth Low Energy (BLE) [8]. The acceleration measurements are key in order to make the different SNs in the WSN more power-efficient. It is important to know when a train is moving and when it has stopped. Based on these two physical parameters, the WSN can be placed in a deep sleep mode or the SNs can be woken up and data can be transferred to a CN. RF measurements illustrate what type of antenna is ideal to deploy in this harsh RF environment, but also what Tx level is ideal to transfer the data in a power efficient way.

In section II the different measurement setups are elaborated followed by the hardware used for these measurements. Next, in section III, measurements are described combined with a brief discussion of these results. Finally, there is a conclusion (section IV) which acceleration measures can be taken and which antenna can be used at what Tx level.

II. Measurement Setup

A. Used hardware

All measurements were performed with the BLE development boards from Silicon Laboratories (SiLabs) containing the multiprotocol ERF32MG13 chip [9]. This System-on-Chip (SoC) contains a radio with a maximum Tx level of $19\,\mathrm{dBm}$ at the frequency of $2.45\,\mathrm{GHz}$, consists of an on-board 32-bit, $38.4\,\mathrm{MHz}$ ARM Cortex M4 microcontroller (MCU) with DSP instruction set. Furthermore, this board has an integrated F-antenna and an U.FL connector. This way, other antennas can easily be connected.

For the RF measurements proposed in subsection II-C, the following two antennas were selected. The first investigated antenna is a dual-band Planar Inverted F-Antenna (PIFA) [10] with a frequency range of $(2.4\text{–}2.5)\,\mathrm{GHz}$ and $(4.9\text{–}6)\,\mathrm{GHz}$,

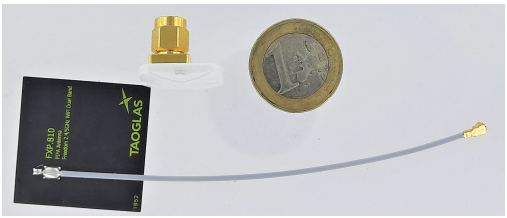

Fig. 1. Picture of the selected antennas with on the left the patch antenna and on the top the button antenna.

with a radiation efficiency of 76 % and 84 % and a maximum gain of 2.4 dBi and 5 dBi, respectively. This antenna is linearly polarized with an almost omnidirectional radiation pattern at 2.45 GHz, which makes it an excellent antenna for BLE. This polymer antenna has an overall size of $31 \times 31 \times 0.1$ mm, as can be seen in Fig. 1 on the left side. We further refer to this as the *'patch'* antenna.

The second investigated antenna is also a PIFA [11] with a frequency range of (2.4–2.5) GHz, a radiation efficiency of 30.6 % and a maximum gain of 0.4 dBi in free space. This antenna is also linear polarized with an almost omnidirectional radiation pattern at 2.45 GHz. This Acrylonitrile Butadiene Styrene (ABS) antenna has an overall size of $19.8 \times 14.3 \times 16.4$ mm, as can be seen in Fig. 1 on the top side. We further refer to this as the *'button'* antenna.

To perform the acceleration measurements of subsection II-B, the ultra-small, low-power, triaxial accelerometer BMA280 [12] was selected. Furthermore, this accelerometer has already been soldered on the development board of SiLabs. This sensor features an integrated low-pass filter with an output data rate up to 500 Hz for an unfiltered input data rate of 2 kHz. Moreover, it possesses a resolution of 4096 LSB/g in the ± 2 g range, can be used in ± 2 g, ± 4 g, ± 8 g and ± 16 g range, communicates via an SPI 3-wire communication link. Moreover, it contains an integrated temperature sensor and multiple interrupts that can be configured to respond on motion events as well as on prolonged motionless conditions. These properties make the accelerometer excellent to detect when a train wagon is moving or not.

B. Acceleration measurement setup

The first setup proposed in this paper is used for acceleration measurements. Here, an accelerometer will be attached to a train wagon and will measure the vibrations of a train wagon that is starting and stopping with or without air brakes.

The accelerometer is mounted on a 3D-printed Polylactic Acid (PLA) mount attached via neodymium magnets to the wagon above the most outer wheel axle, as can be seen in Fig. 2 and Fig. 3. PLA is a hard plastic so in combination with the large neodymium magnets, the accelerometer will measure the train vibrations and the damping effect can be neglected. This way, the X-axis (a_x) of the accelerometer is perpendicular towards the wheel axle of the train wagon, for measuring the gravitational force. The Y-axis (a_y) is alongside the train wagon, for measuring the movement of the wagon. The Z-axis (a_z) is in line with the wheel axle of the train wagon, for measuring left or right movements.

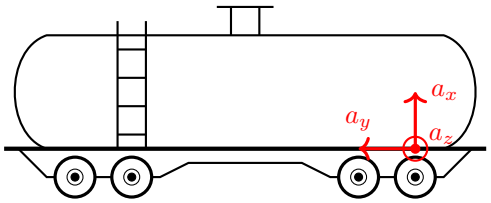

Fig. 2. Acceleration measurement set up. The train wagon is equipped with an accelerometer attached via a 3D-printed PLA mount to the frame above the outermost wheel axle.

Fig. 3. Accelerometer attached to the container train wagon above the most outer wheel axle.

C. RF measurement setup

The second proposed setup consists of Received Signal Strength Indicator (RSSI) measurements. The main purpose of these measurements is to find the optimal Tx level of a BLE node that is sending sensor data towards an CN also mounted on the train wagon.

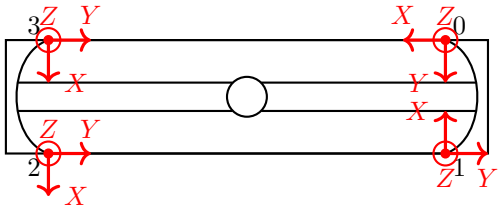

Fig. 4. Top view representation of the RF measurement set-up on the tank wagon. The four corners are labeled from 0 to 3. At 0 a Tx node is placed, while at 1, 2 and 3 an Rx node is placed.

Fig. 4 illustrates the measurement setup, where a top view of a train wagon can be seen. A Tx node is placed at position 0 and a RX node is placed at positions 1, 2 and 3, respectively. From position 0 to 1, there is a clear Line-Of-Sight (LOS) link, although with a lot of metal in the vicinity. From position 0 to 2, there is no LOS, and a large empty or full metal tank can shadow the communication link. From position 0 to 3, there is no LOS, but due to the position of the transmitter and receiver, there can be less obstruction when compared to the link from position 0 to 2.

The Tx node is programmed to send 300 coded advertisement packages with an interval of 20 ms at a certain Tx level ranging from (0–10) dBm in steps of 1 dBm. Due to battery

Fig. 5. Rx node attached at position 2 on the tank wagon.

management reasons, a Tx level of more than 10 dBm is not measured. The advertisement packages are labelled in the data, in order to prevent erroneous data capturing of other nodes. The Rx node was programmed to continuously scan for these coded advertisement packets, but also to log the RSSI level and to count the amount of received packages at a certain Tx level. Both nodes were mounted on a 3D-printed PLA mount with an integrated neodymium magnet. Fig. 5 illustrates the Rx node attached on the wagon at position 2.

III. Measurements & Discussion

A. Acceleration measurements

With the acceleration, the vibration of the train wagon in the moving direction is measured. These measurements are used to calculate the Signal Magnitude Vector (SMV) as follows.

$$SMV = \sqrt{a_X^2 + a_Y^2 + a_Z^2} \tag{1}$$

The measurements are performed on a train, composed of a small locomotive and two different wagons. The first one was a container and the second one a tank, both empty.

1) Wagon stopped: Efficiently employing the low-power and sleep modes of the WSN can drastically extend the battery lifetime. Instead of a battery-intensive continuous scan by the MCU, the system is mostly placed into a deep sleep mode and is only woken up by accelerometer events, if a train movement is detected. As mentioned earlier, the BMA280 has several built-in interrupts which are very useful.

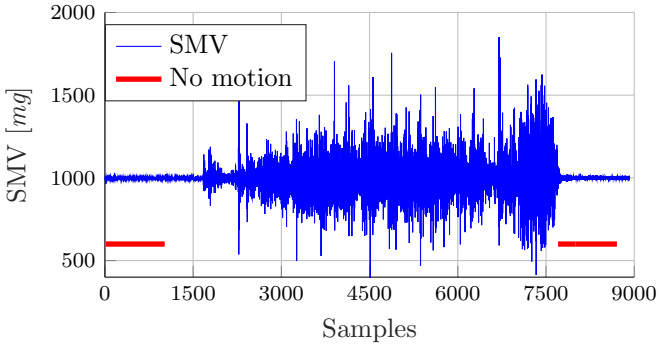

Fig. 6. No motion interrupt result based on vibrations measured on the first wagon, with air brakes.

Fig. 6 illustrates the vibration of the container wagon measured at a sample rate of 4 ms. To find out if the train has stopped, the *no motion interrupt* is selected. An interrupt is triggered when the slope of all selected axes is smaller than the predefined threshold for a certain time slot or a consecutive amount of samples. The red lines in Fig. 6 show the result of the *no motion interrupt*. The parameters of this interrupt are a time slot of 4 s or 1000 consecutive samples and a slope difference of 100 *mg*. It can be stated that this interrupt performs as desired. A larger time slot will prevent the MCU from waking up too fast in case the wagon stopped without air brakes.

2) Is the train moving?: Secondly, knowing when the train is moving, is important to put the WSN in a deep sleep mode until the train stopped and a *no motion interrupt* is triggered. The BMA280 has two built-in interrupts that can be utilized.

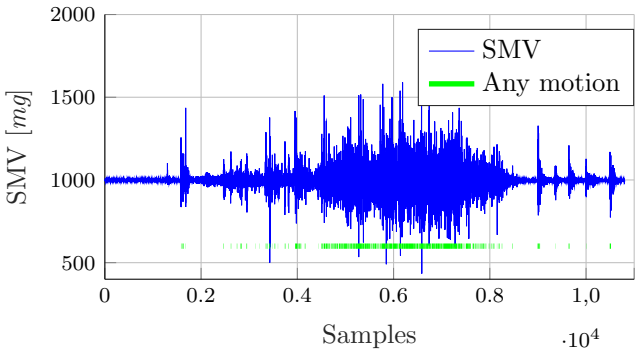

Fig. 7. Any motion interrupt result based on vibrations measured on the first wagon, no air brakes.

The *any motion interrupt* is triggered if the slope difference of the selected axes for a certain amount of consecutive samples is larger than a predefined threshold. Fig. 7 illustrates the 473 alerts that are triggered on the measured vibration of the container wagon not utilizing air brakes, sampled at a rate of 4 ms. The parameters of this interrupt are a time slot of 16 ms or 4 consecutive samples and a slope difference of 50 *mg* is used.

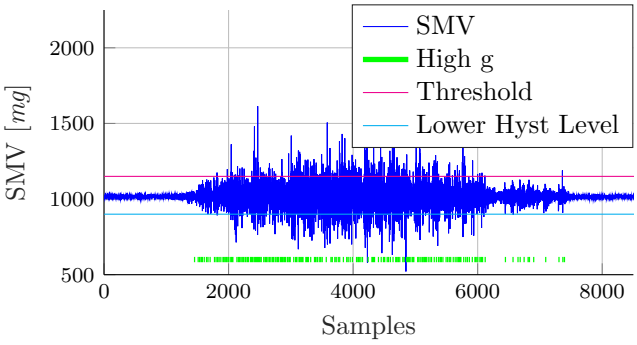

Fig. 8. High-g interrupt result based on vibrations measured on the second wagon, with air brakes.

A second possible interrupt is called *High-g interrupt*. This interrupt is triggered if the absolute value of one of the selected

axis ('or' relation) is higher than a predefined threshold for at least the defined time slot. The interrupt is cleared when the absolute value of all axis ('and' relation) is lower than the threshold minus the lower hysteresis level for the defined time slot.

Fig. 8 illustrates the vibrations measured on the second wagon sampled at a sample rate of 4 ms and when braking with air brakes. The parameters of the interrupt are a time slot of 80 ms or 20 consecutive samples, a threshold on 1150 *mg* (purple line) and a lower hysteresis level of 250 *mg* (cyan line). This results in 168 triggered interrupts. This clearly illustrates that both interrupts can be used to place the WSN in a deep sleep mode very efficiently. Since the accelerometer has a current consumption of 130 µA in normal mode, the influence on the battery lifetime is minimal. Furthermore, it can be noticed that the measured peaks are smaller on the second wagon, but still measurable.

3) Air brakes: Based on measurements, braking with or without air has less influence on the measured SMV. Fig. 6 and Fig. 7 illustrate the vibrations measured from the container wagon that is braking with and without air brakes, respectively. One can clearly see that after the wagon stops without air brakes, it results in decreasing repetitive shocks from the hydraulic absorbers. Most of these are perfectly measurable and do not have an influence on the WSN or the measurements these sensors make. With air brakes, it results in a smooth full stop. However, as soon as the brakes were released, some small aftershocks were noticed.

B. RF Measurement

The RF measurements consist of logging the RSSI level and the amount of received packages at a certain Tx level. In post-processing, the Average Received Power (ARP) and the Package Receive Rate (PRR) are calculated, as follows.

$$ARP_{TX}\,[\mathrm{dB}] = 10.\log_{10}\left(\frac{1}{m}.\sum_{n=1}^{m} 10^{\frac{RSSI_n\,[\mathrm{dB}]}{10}}\right) \quad (2)$$

$$PRR_{TX}\,[\%] = \frac{m}{300} \quad (3)$$

m = number of received packets

1) Reference measurements: As reference measurement, the Rx and Tx node were placed in the anechoic chamber with a distance of approximately 3.5 m between both nodes. Fig. 9 illustrates the ARP for three different situations: two patch antennas as Tx and Rx node, a button antenna as Tx node and a patch antenna as Rx node and two button antennas as Tx and Rx node. This result clearly proves that the patch-patch combination gives the highest ARP and hence has the best reception. The combinations with the button antenna results in weaker signals down to sometimes unusable reception. For the button-button link no values were received between (0–5) dBm, because the corresponding ARPs are lower than the minimal Rx sensitivity of the MCU. Fig. 10 shows the PRR, where the same conclusion can be drawn. Based on these results, the button-patch link results in a good quality reception although with very low received power levels. Therefore, the link margin is limited.

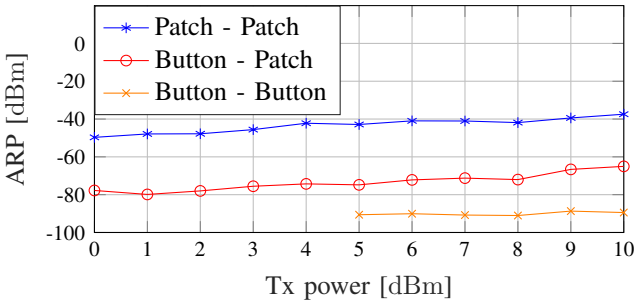

Fig. 9. ARP: reference measurement in the anechoic chamber.

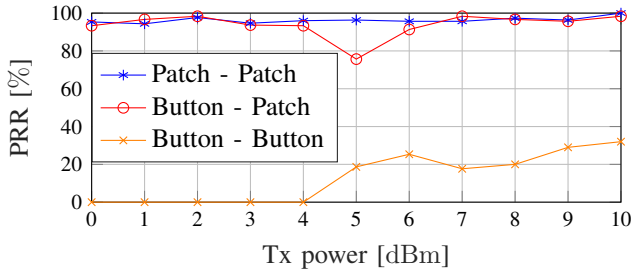

Fig. 10. PRR: reference measurement in the anechoic chamber.

2) Real-life measurements: Based on the measurements performed in the anechoic chamber, it can be stated that the button antenna has a worse performance. To confirm this statement, the measurements were repeated in real-life. Fig. 11 and Fig. 12 illustrate the ARP and PRR on a full tank wagon. In order to see how the antenna link performs in the worse condition, the Tx node was placed at position 0 and the Rx node was placed on position 2. Fig. 11 illustrates that the ARP level of the button-button and button-patch link are lower than the minimum Rx sensitivity level of −94.6 dBm from the radio integrated in the MCU. Fig. 12 proves that no packets were received for those links. Therefore, the patch-patch antenna link was selected to perform the other measurements.

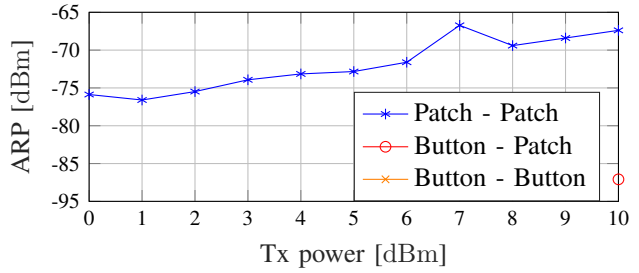

Fig. 11. ARP: full tank wagon for the different antenna links.

Fig. 13 illustrates the ARP on an empty tank wagon. From position 0 to 1, we have a better performance compared to

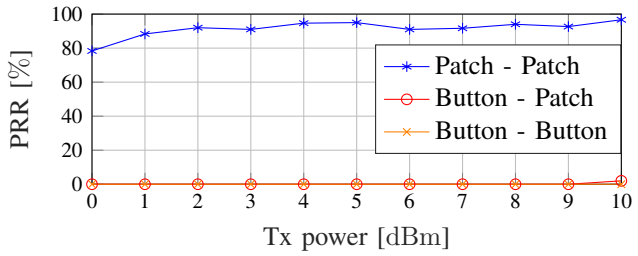

Fig. 12. PRR: full tank wagon for the different antenna links.

the reference measurement because the measurement distance between the nodes is smaller. From position 0 to 2 or 3, there is a serious decrease in received power, but still enough to have a good communication between both nodes. Fig. 14 illustrates the PRR for the empty tank wagon. The same conclusion can be drawn for the position 0 to 1 link. From position 0 to 2, there is a good reception, although metal structures of the train wagon need to be taken into account. Starting from 2 dBm transmit power, an ARP of around -82 dBm and a PRR of approximately 65 % are measured. From position 0 to 3, there is some fluctuation, probably due to multipath effects. Based on the performed measurements, we can conclude that the patch-patch link performs well even when a large metal structure is in close proximity. This is due to the properties of the employed antenna, more importantly the omnidirectional radiation at a frequency of 2.45 GHz of the patch antenna.

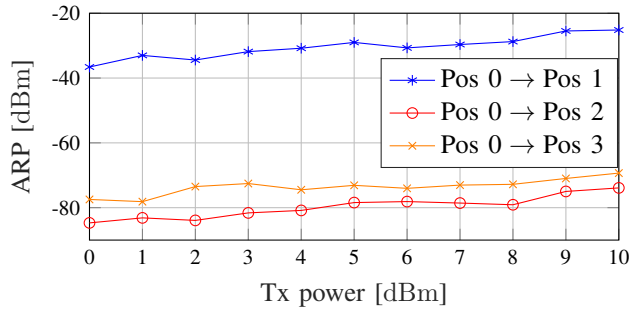

Fig. 13. ARP: patch-patch link on an empty tank wagon.

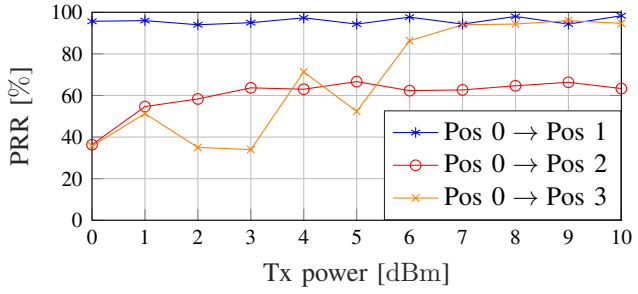

Fig. 14. PRR: patch-patch link on an empty tank wagon.

Fig. 15 presents the measured results for the ARP and Fig. 16 for the PRR on another tank wagon, completely filled. The same conclusion can be drawn, but with a better performance. For the worst communication link 0 to 2, starting from a Tx power level of 2 dBm, there is a PRR of 90 % and an ARP of approximately -75 dBm. From position 0 to 2, an increase of approximately 5 dBm ARP level and 50 % PRR is observed. Furthermore, compared to the results of Fig. 13 and 14, it can be concluded that the fluid has a positive effect on both the ARP and PRR. This can result in a decrease of Tx power and hence a longer battery life when used in practical applications.

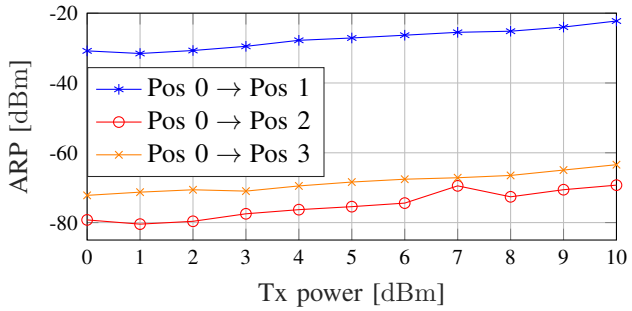

Fig. 15. ARP: patch-patch link on a full tank wagon.

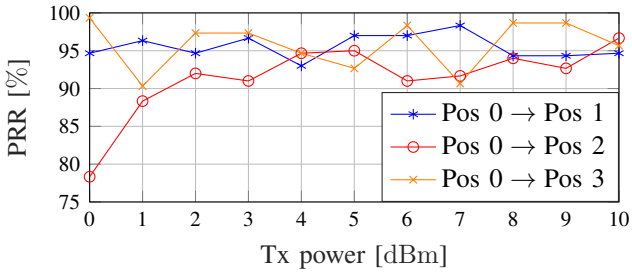

Fig. 16. PRR: patch-patch link on a full tank wagon.

3) Brakes: In a next step, the nodes were placed on the outside of the brakes of the tank wagon. At each side, the wagon has four steel wheels, each having their own brake pair. The node was always placed on the most outer wheel brake, as can be seen in Fig. 17. Fig. 18 and Fig. 19 show the results for the ARP and PRR on an empty tank wagon brakes, respectively. From brake 1 to 2, there is an ARP level ranging from -75 dBm to -65 dBm and a PRR of 95 %. This illustrates that reliable communication is possible.

From brake position 0 to 2, similar results were measured, so the same conclusion can be drawn. It is important to mention that during these measurements, the nodes were attached in front of the big steel wheels. Therefore, from position brake 0 to 2, the RF signals encounter at least two large metal structures. From the central node to 2, the received signal levels decrease. This is because the signals are close to the big metal plate underneath the tank wagon as well as the steel wheels. As conclusion, starting from a Tx level of 4 dBm an average PRR of approximately 92 % is measured and an ARP of around -83 dBm is measured.

Fig. 17. Rx node placed on the outer wheel brake.

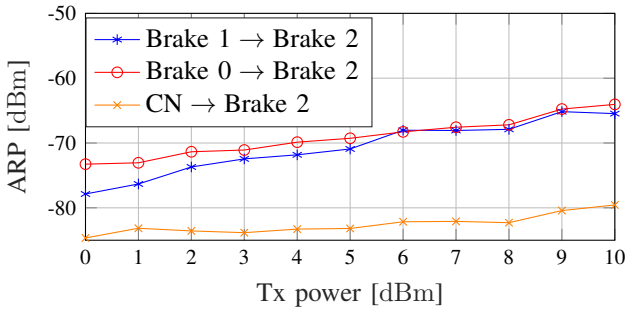

Fig. 18. ARP: from the outer brake on an empty wagon.

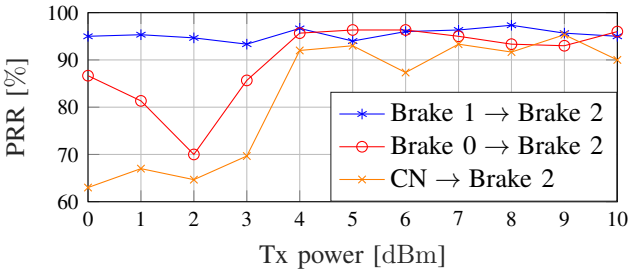

Fig. 19. PRR: from the outer brake on an empty wagon.

IV. Conclusion

This paper presents the possibilities to use an accelerometer to put a WSN in a deep sleep mode or to wake up the system when connected to an industrial IoT network. Furthermore, it proposes a low cost, easy producible and commercially available PIFA antenna that works perfectly in these harsh metal environments train wagon are.

The first set measurements introduced in this paper were acceleration measurements. These were obtained on different train wagon types, braking with or without air brakes. Based on these measurements and the built-in interrupts from the BMA280, a WSN on the train wagon can easily be put to sleep or wake up. Employing the no motion, any motion and high-g built-in interrupts of the accelerometer, the movements of the train can be easily monitored and the WSN can be put to sleep or wake up. This will have a large impact on the battery lifetime of each SN. Furthermore, it can be concluded that there is a small difference between braking with or without air brakes, but no large impact on the measured vibrations or selected interrupt have been observed.

The second set of measurements introduced, were the RF measurements. Two prefabricated PIFAs were placed on a train wagon, to measure the RSSI levels at different Tx levels. Afterwards, the PRR and ARP were calculated. This illustrated that the first selected patch antenna performs best in every position on the train wagon. In a final step, the patch antenna was placed on the outer brakes and outer wheels of the wagon. Despite the large amount of metal structures, the antenna kept performing in a desirable way.

These measurements also illustrate that there are limited differences between a full or empty tank wagon. Starting from a Tx level of $2\,\mathrm{dBm}$, there is an PRR of $90\,\%$ and an ARP of approximately $-75\,\mathrm{dBm}$ on a full tank wagon. On an empty tank wagon, less favorable, but still usable results were registered. The measurement on the brakes of the empty train wagon clearly illustrated that reliable communication is possible. Starting from a Tx level of $4\,\mathrm{dBm}$ an average PRR of $\pm 92\,\%$ is measured and an ARP of around $-83\,\mathrm{dBm}$ is measured.

References

[1] U. Biaou, S. Iben Jellal, M. Bocquet, S. Baranowski, A. Rivenq, and P. Mariage, "Study of the Positioning of Wireless Sensors for Communication at 2.4 GHz Inside the Train," in *2017 International Conference on Wireless Technologies, Embedded and Intelligent Systems (WITS)*, 2017, pp. 1–5.

[2] N. Barkovskis, A. Salmins, K. Ozols, M. A. Moreno García, and F. P. Ayuso, "WSN Based on Accelerometer, GPS and RSSI Measurements for Train Integrity Monitoring," in *2017 4th International Conference on Control, Decision and Information Technologies (CoDIT)*, 2017, pp. 0662–0667.

[3] A. Lo Schiavo, "Fully Autonomous Wireless Sensor Network for Freight Wagon Monitoring," *IEEE Sensors Journal*, vol. 16, no. 24, pp. 9053–9063, 2016.

[4] M. T. Lazarescu and P. Poolad, "Asynchronous Resilient Wireless Sensor Network for Train Integrity Monitoring," *IEEE Internet of Things Journal*, vol. 8, no. 5, pp. 3939–3954, 2021.

[5] M. Soliman, Y. Dawoud, E. Staudinger, S. Sand, A. Schuetz, and A. Dekorsy, "Influences of Train Wagon Vibrations on the MmWave Wagon-to-Wagon Channel," in *12th European Conference on Antennas and Propagation (EuCAP 2018)*, 2018, pp. 1–5.

[6] Y. Gong, S. Wang, Z. Xie, T. Zhang, W. Chen, X. Lu, Q. Zeng, Y. Gao, and W. Huang, "Self-Powered Wireless Sensor Node for Smart Railway Axle Box Bearing via a Variable Reluctance Energy Harvesting System," *IEEE Transactions on Instrumentation and Measurement*, vol. 70, pp. 1–11, 2021.

[7] L. Wang, T. He, Z. Zhang, L. Zhao, C. Lee, G. Luo, Q. Mao, P. Yang, Q. Lin, X. Li, R. Maeda, and Z. Jiang, "Self-sustained autonomous wireless sensing based on a hybridized TENG and PEG vibration mechanism," *Nano Energy*, vol. 80, p. 105555, 2021. [Online]. Available: https://www.sciencedirect.com/science/article/pii/S2211285520311290

[8] S. L. Oliva, A. Palmieri, L. Invidia, L. Patrono, and P. Rametta, "Rapid Prototyping of a Star Topology Network based on Bluetooth Low Energy Technology," in *2018 3rd International Conference on Smart and Sustainable Technologies (SpliTech)*, 2018, pp. 1–6.

[9] Silicon Laboratories, "EFR32MG13 Series 1 Modules," www.silabs.com, accessed on July 13, 2022.

[10] Taoglas, "Freedom FXP810 2.4/(4.9–6.0) GHz Flex PCB Antenna, 100 mm, I-PEX MHF® I (U.FL)," www.taoglas.com, accessed on July 13, 2022.

[11] ——, "WCM.01.0151W 2.4 GHz Button Antenna," www.taoglas.com, accessed on July 13, 2022.

[12] Bosch Sensortech, "Acceleration Sensor BMA280," www.bosch-sensortec.com, accessed on July 13, 2022.

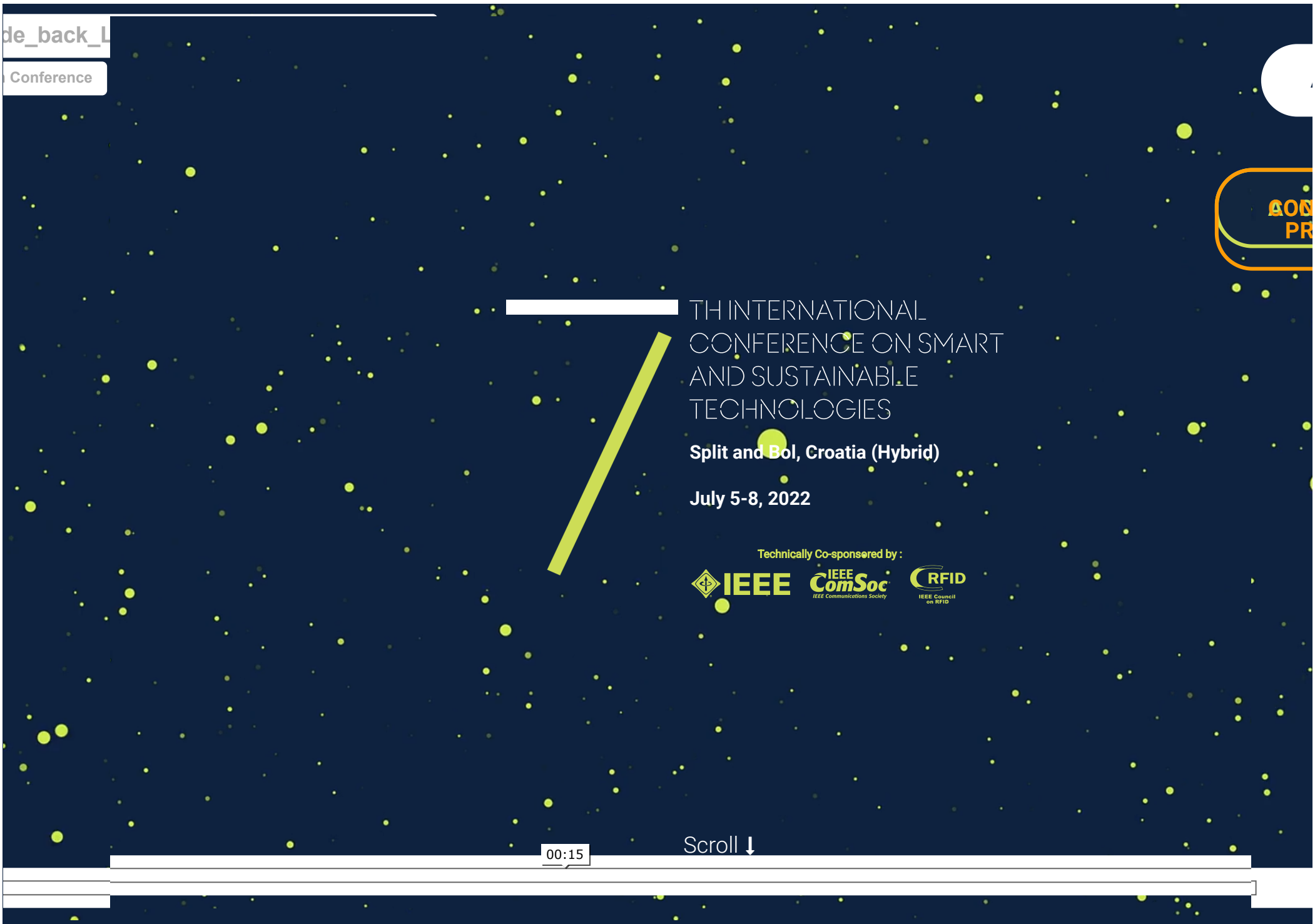

VIRTUAL ACCESS to the SpliTech 2022 Conference

SpliTech 2022 Conference is held in Hybrid form – live in the hotel Elaphusa, Bol (island of Brač), Croatia, with virtual access through the web platform.

To get the best experience possible for SpliTech we advise you to connect through the following link:

SpliTech 2022 VIRTUAL PLATFORM

Instructions for presenting on SpliTech 2022 can be found on the following link: https://2022.splitech.org/wp-content/uploads/2022/07/Splitech-2022-App-Manual.pdf
All “virtual” authors are encouraged to present the paper in real – time connecting to the streaming link within the app.

The video is included as a part of the back – up and can be shared for cases of connection problems. Also, videos can be available for watching later to catch up with some “missed” talks due to the parallel sessions.

All presenting (VIRTUAL) authors are, however, required to be connected to their session, to be available for the Q&A’s.

Conference technical support team is available for assistance in case of any uncertainities.

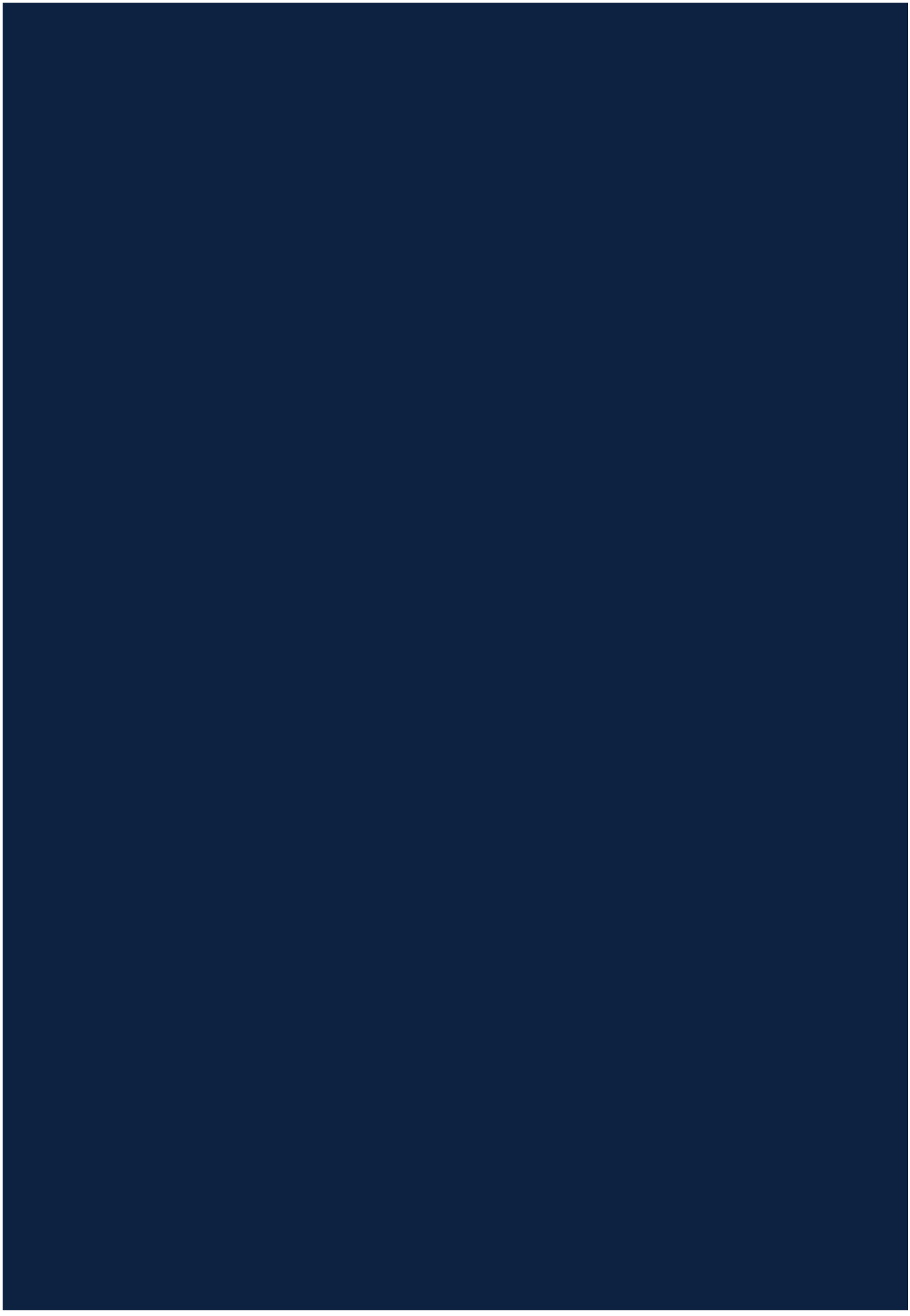

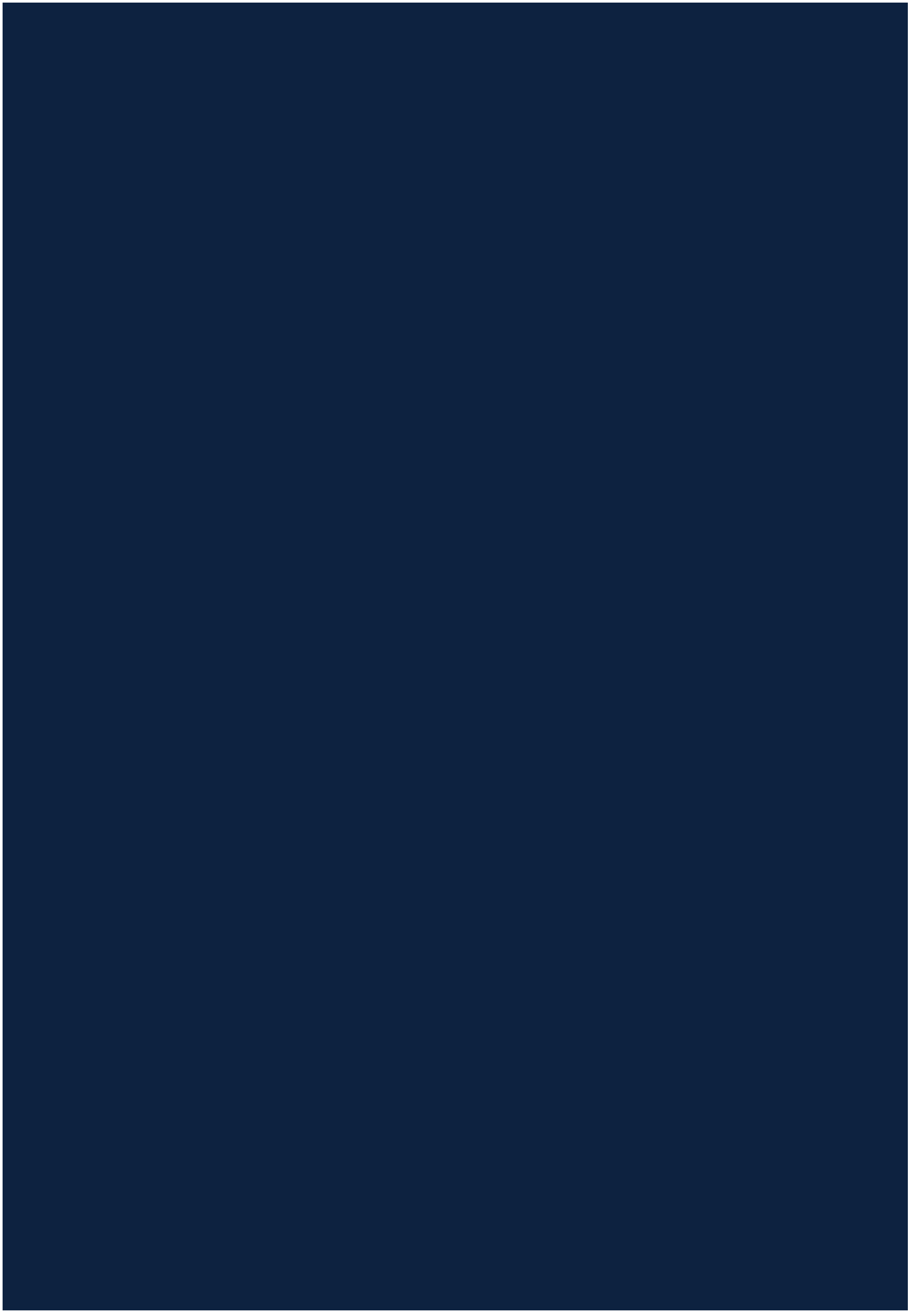

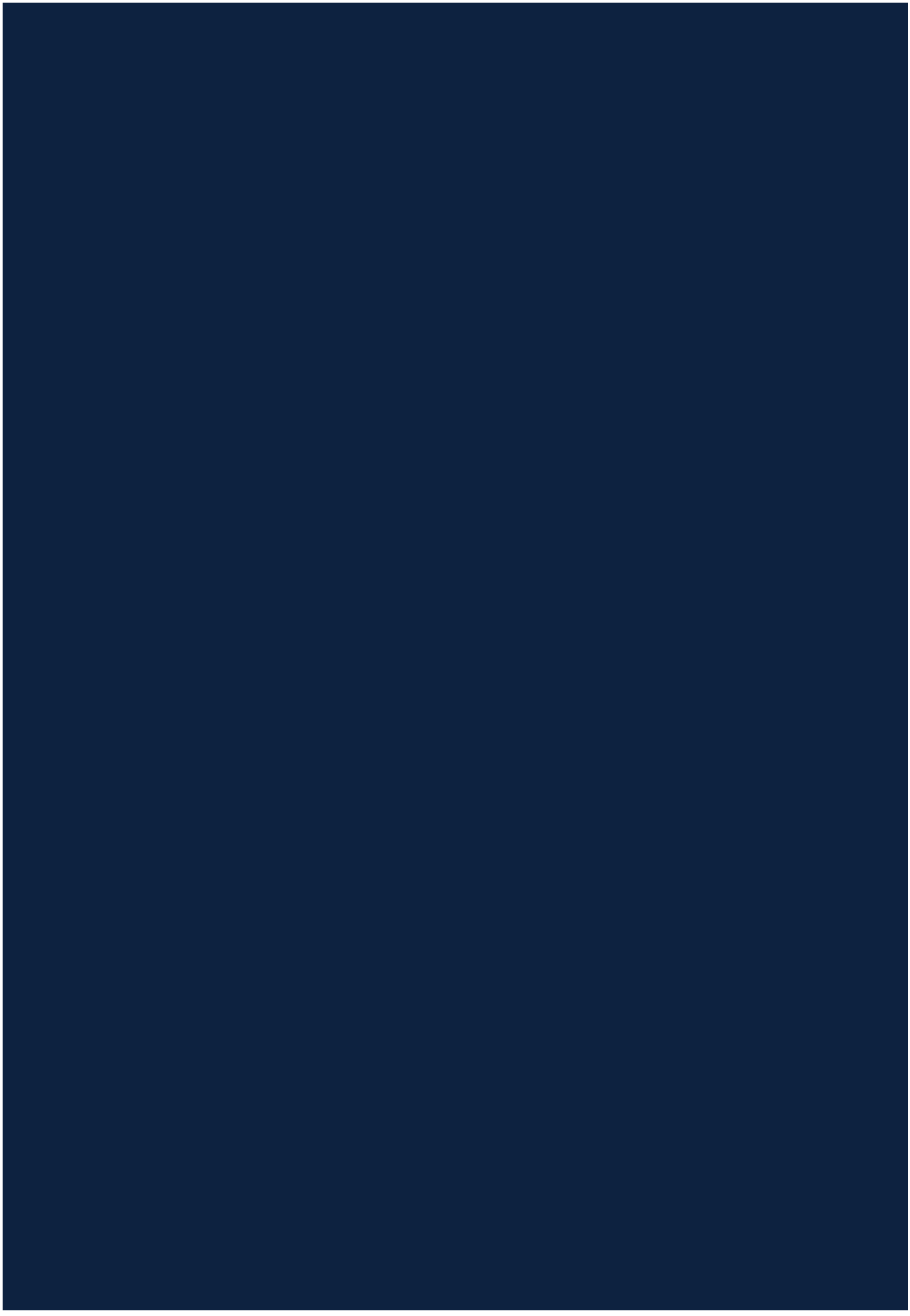

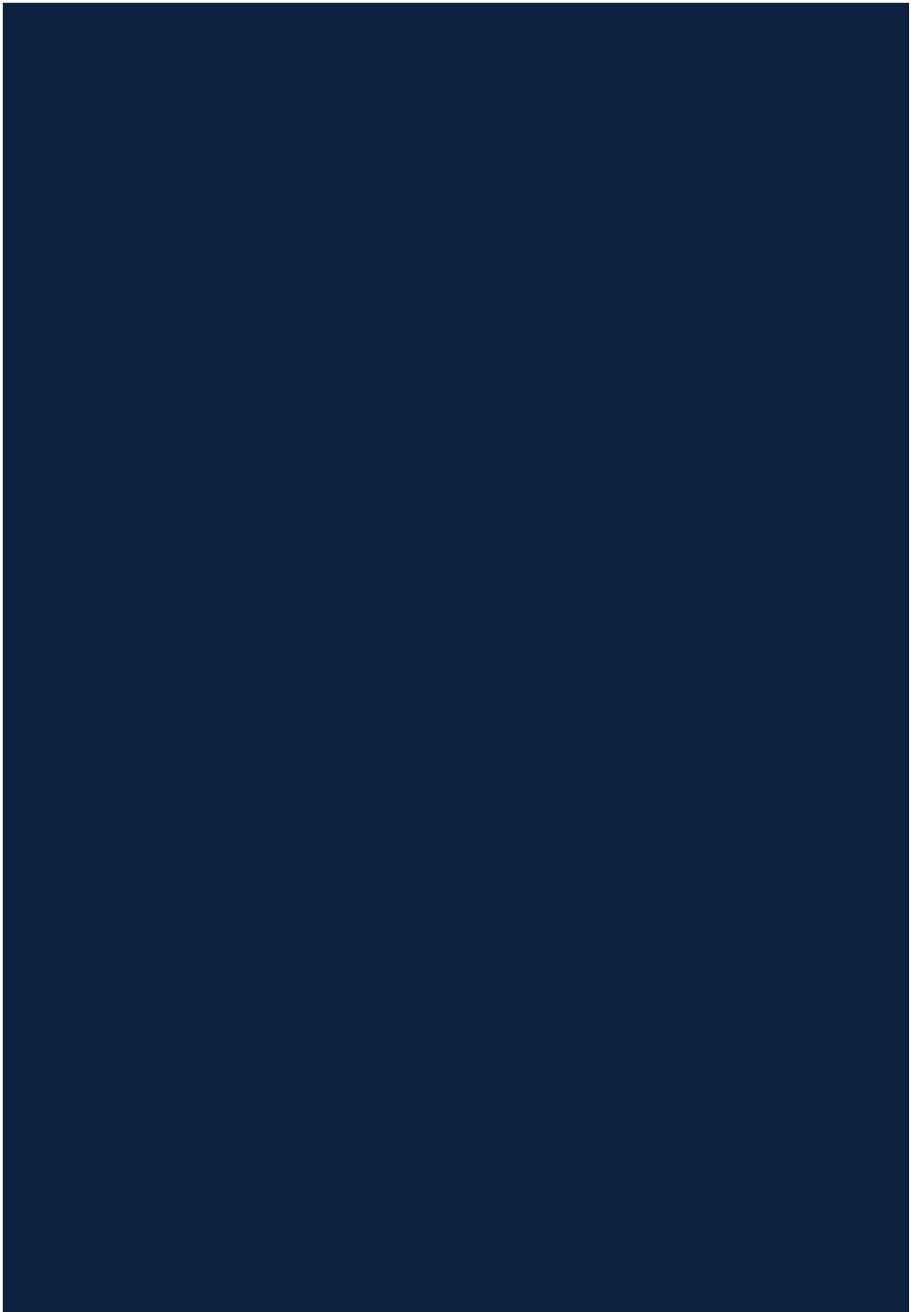

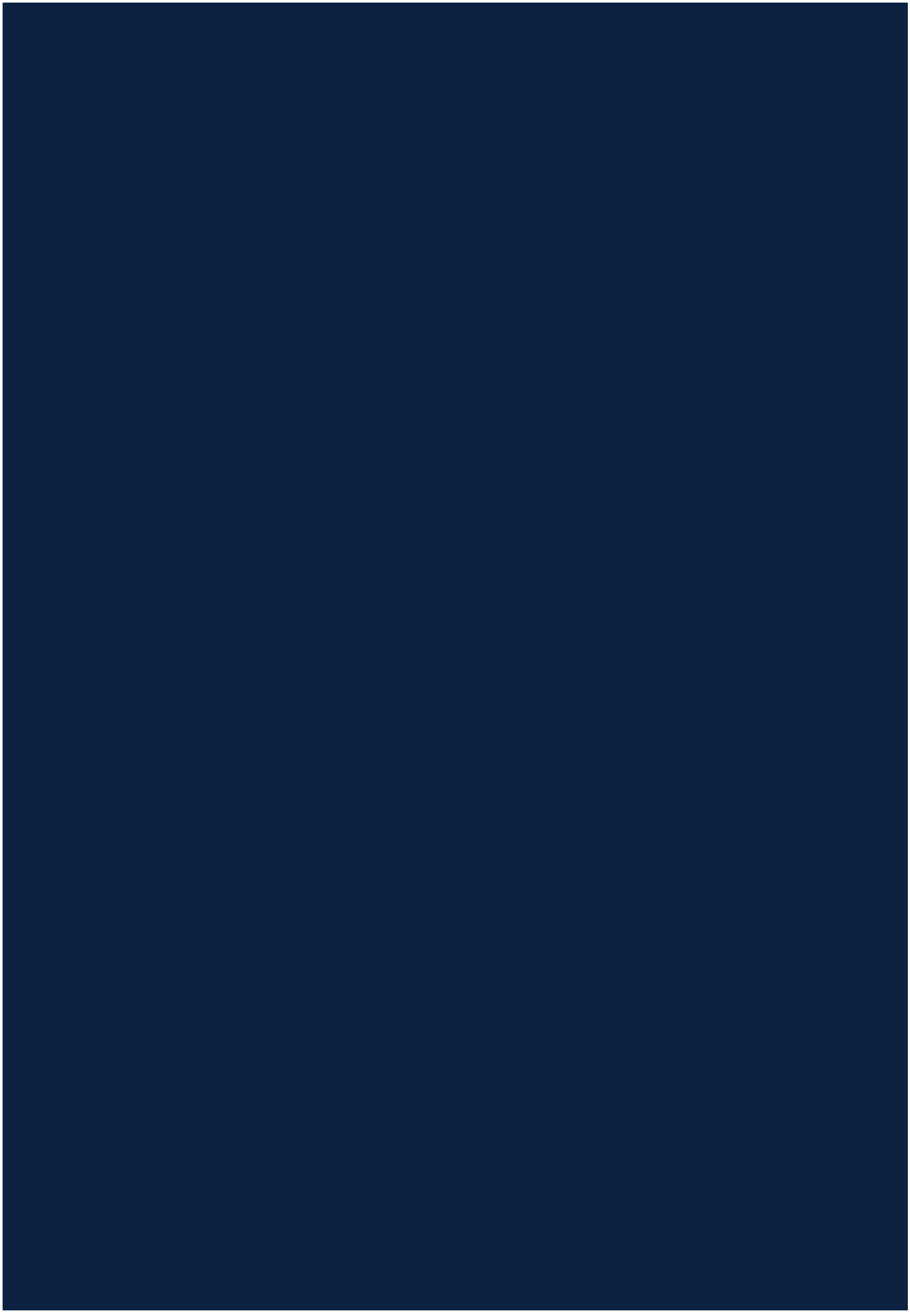

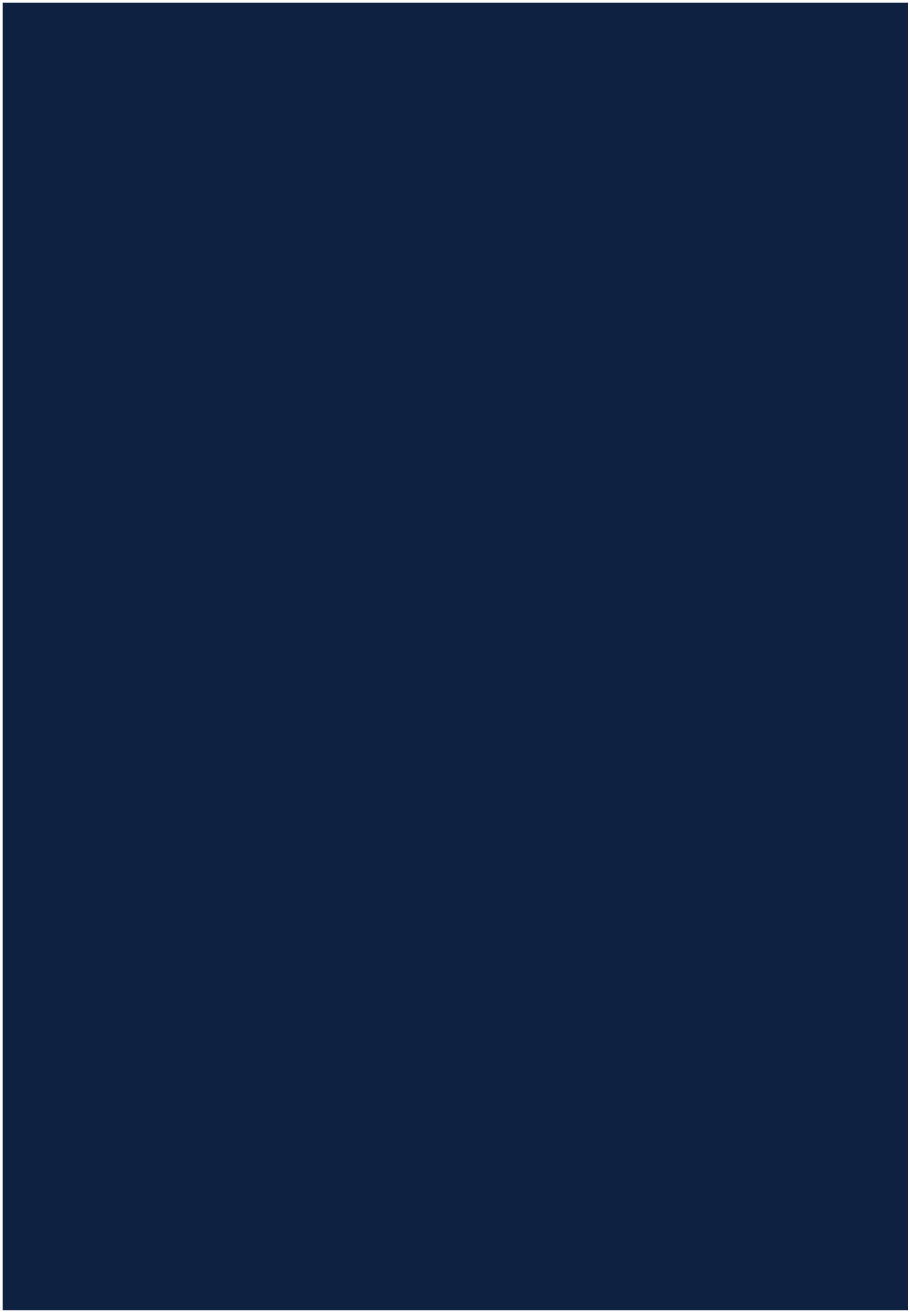

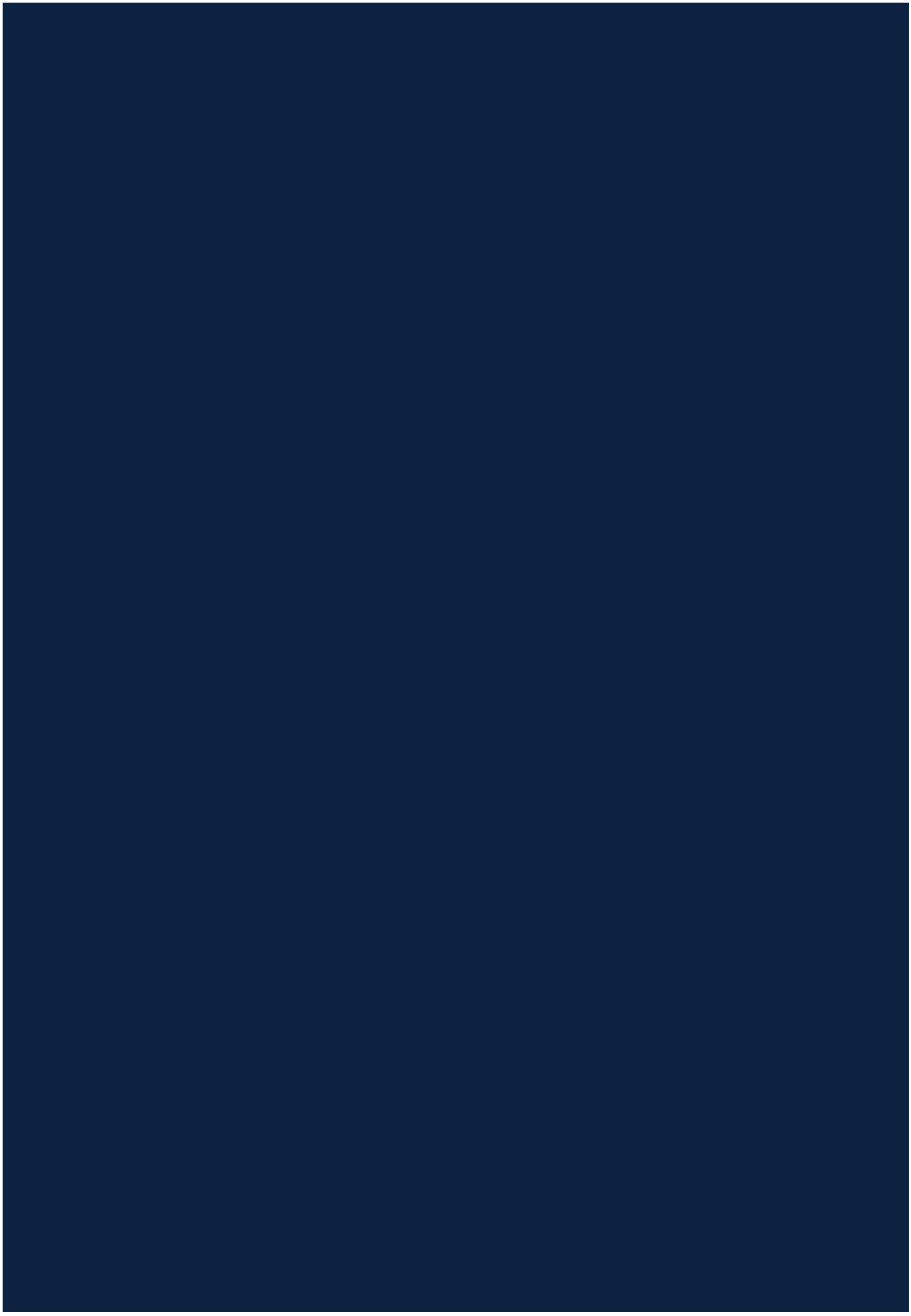

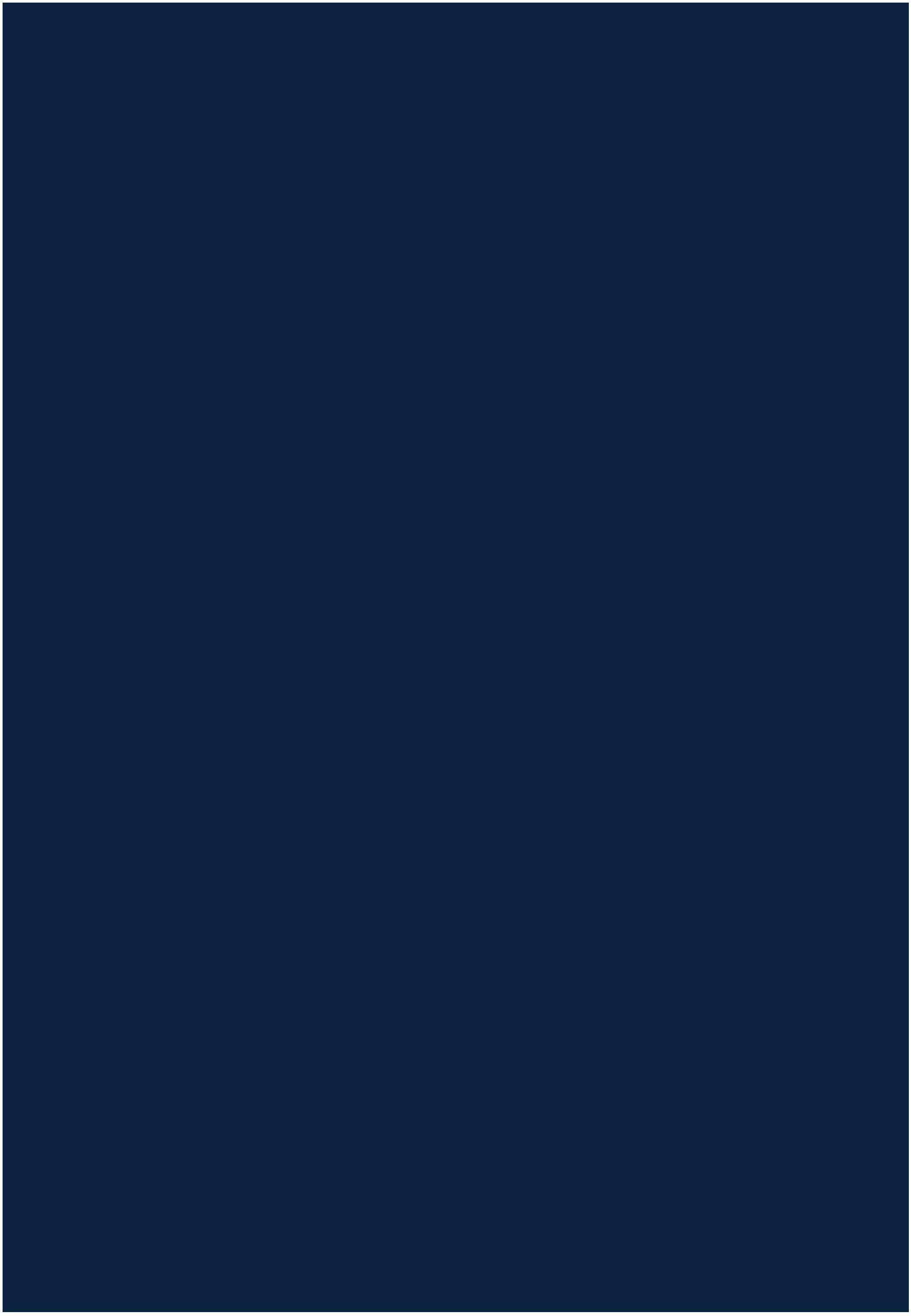

REGISTRATION

ACADEMIA MEMBERS

€ 470

after June 1 2022 – 570 €

- Access to all events
- Bag of goodies
- Gala dinner voucher
- Social events
- USB Proceedings
- Lunches and Refreshments during the conference

Book Your Ticket

INDUSTRY MEMBERS

€ 470

after June 1 2022 – 570 €

- Access to all events
- Bag of goodies
- Gala dinner voucher
- Social events
- USB Proceedings
- Lunches and Refreshments during the conference

Book Your Ticket

STUDENT MEMBERS *

€ 270

after June 1 2022 – 370 €

- Access to all events
- Bag of goodies
- Gala dinner voucher
- Social events
- USB Proceedings
- Lunches and Refreshments during the conference

Book Your Ticket

* for paper registrations, applicable only if the paper is authored by students-only

- Prices are defined for live participation. In the case of a virtual conference attendance, 20 % discount will be applied to Academia and Industry Members, 30 % discount will be applied to Student Members

ORGANIZATION

FESB

UNIVERSITY OF SPLIT SCHOOL OF MEDICINE

ICT ŽUPANIJA SPLITSKO-DALMATINSKA

SPONSORS

IDENTIV

MESSER

ion solutions

rudan
UČINKOVITO UPRAVLJANJE ENERGENTIMA

Rita Solar

LAB ID

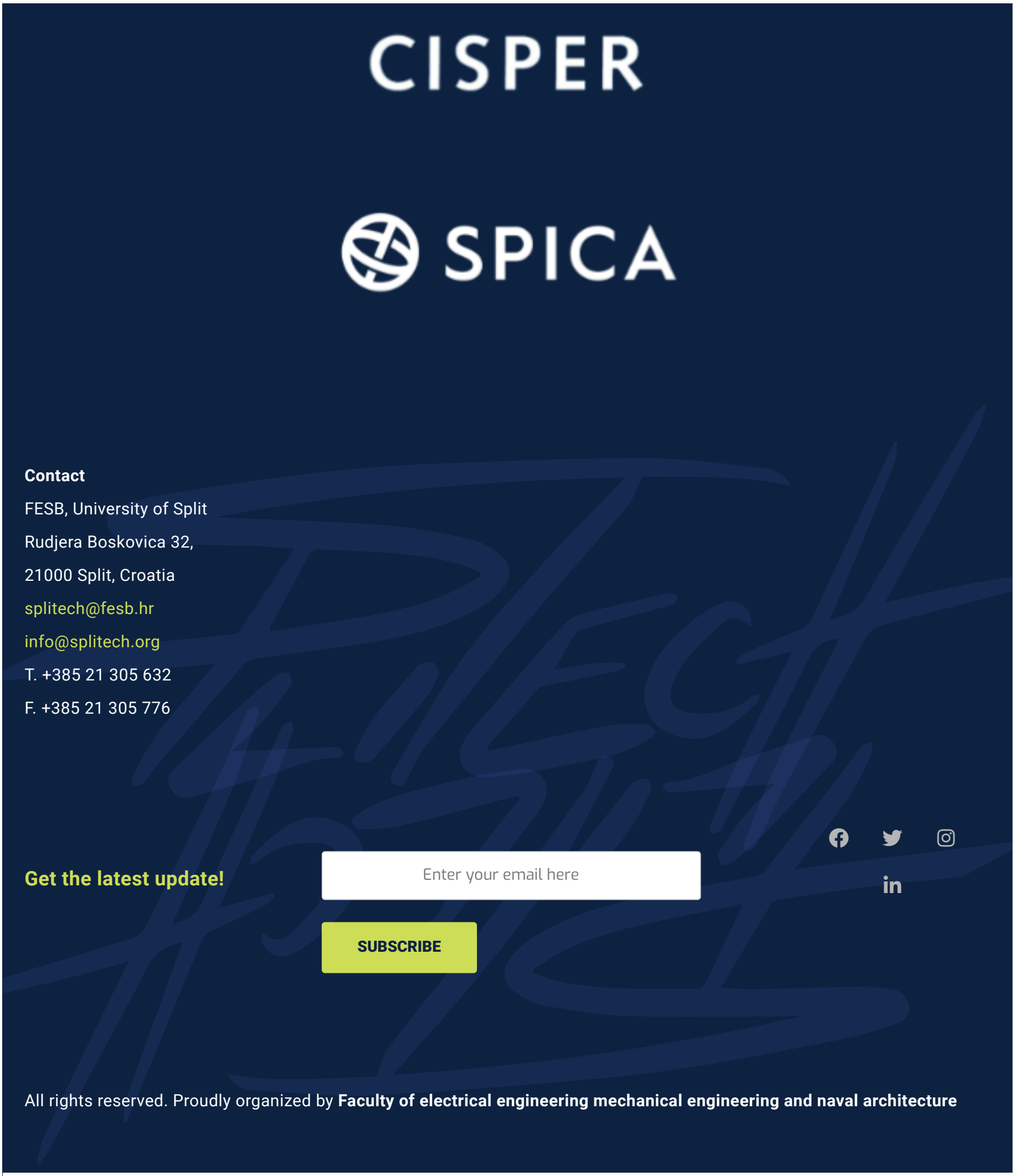
CISPER
SPICA
Contact
FESB, University of Split
Rudjera Boskovica 32,
21000 Split, Croatia
splitech@fesb.hr
info@splitech.org
T. +385 21 305 632
F. +385 21 305 776
Get the latest update!
Enter your email here
SUBSCRIBE
All rights reserved. Proudly organized by Faculty of electrical engineering mechanical engineering and naval architecture